



Optimization of biofuel synthesis from used food oil by transesterification

Sadjia Bertouche^{a,*}, Naima Sahraoui^a, Nassila Sabba^a, Nesrine Ayad^b

^aLaboratory of Matter's Valorization and Recycling of Materials for Sustainable Development (VRMDD), University of Sciences and Technology Houari Boumediene, El Alia BP32, 16111, Bab Ezzouar, Alger, Algeria, email: bertouche.sadjia@gmail.com

^bEcole supérieure du matériel Defunt moudjahid EL-CHEIKH AMOUD BEN EL-MOKHTAR, Alger, Algérie

Received 30 June 2022; Accepted 6 October 2022

ABSTRACT

The objective of this experimental work was to synthesize biofuels from used food oils by a transesterification chemical process. The influence of the parameters affecting the yield of the transesterification reaction were assessed and consequently optimized to obtain good quality biodiesel, with an optimal conversion. Their chemical composition and calorific value make biofuels good alternatives to fossil fuels. To make them compatible with engines, some transformations are required to decrease their viscosity and improve their properties. The processes and their parameters were optimized by experimental methods and the produced fuels were characterized with respect to European Norms (EN 14214). The results of the investigation showed that the best yield is obtained using a mass of CaO = 0.895 g, a temperature = 40°C and a reaction time = 68.85 h.

Keywords: Used frying oils; Transesterification; Biodiesel; Bio-fuels; Diesel engines; Experiments planning method

1. Introduction

The world population has evolved from 2.5 billion in 1950 to 6 billion in 2000 and will reach 9 billion in 2050 according to the studies made by the UN [1]. These demographic changes as well as a higher global standard of living have caused greater consumption rates of goods. This has resulted in enormous energy needs, and huge quantities of waste products that are difficult to manage [2]. A key challenge is how to meet future global energy needs as the world's reserves of oil are limited. Indeed, the most optimistic scenarios predict that peak oil production will be reached between 2028 and 2030 [3]. This assessment includes high-tech oil (i.e., oil that requires advanced technologies to be exploited). The most pessimistic scenarios indicated that this peak was already reached in 2010 and that production has been gradually declining [4]. It can be argued that it is imperative to direct the world's energy consumption towards new clean and renewable resources. Hence the need to look for new fuels that can replace oil in vehicles [5].

Biomass biofuels appear to be one of the best solutions to meet current and short-term energy needs. Increasing the value of biomass has become popular, especially for raw materials of a carbohydrate nature such as cereals, sugar beet and sugar cane, lignocellulosic such as wood, straw, and fodder and oleaginous vegetable oils [6–9]. However, the production of biofuels from these food sources can lead to a shortage and an increase in the prices of these raw materials. The food market expanded significantly between 2002 and 2008 with the price of food increasing by 130%; the production of biofuels was responsible for 75% of this cost rise [7]. It is necessary to focus research on the production of second and third generation biodiesels, while avoiding first generation biofuels considered as an energy source [9,10]. To overcome these problems, researchers are currently studying new ways to produce biodiesel from used food oils [11–14]. Indeed, the usage of old frying oil, slaughterhouse fat, and fish oil is very ecofriendly [15–17].

The main objective of this experimental work was to synthesize biofuels from used food oils by a transesterification

* Corresponding author.

chemical process known. The influence of the parameters affecting the yield of the transesterification reaction were assessed and optimized to obtain a good quality biodiesel, with an optimal conversion.

2. Materials and methods

2.1. Raw materials

The used frying oil utilized in this study was collected from a restaurant in Algiers, Algeria. The oil was carefully filtered and cleaned of all residues. The catalyst employed was lime, of commercial type purchased with granulometry < 1 mm.

2.2. Analysis and characterization

2.2.1. Used frying oil characterization

The physicochemical characterization of the oil was based on the density by the ASTM D70 standard, the viscosity by the ASTM D445 standard, the acidity index by the ISO 660 standard, the calorific value by the ASTM D240 standard, the peroxide index by the NF ISO 3960 standard, the refractive index by the NF ISO 6320 standard as well as the flash point, cloudiness, flow: NF T60-103, ISO 3015:1992, NF T60-105 standard respectively [18–26].

Fourier-transform infrared spectroscopy (FTIR) allows for highlighting the electronic and structural changes that occur at the molecular level. The characterization was carried out qualitatively using a Fourier transform infrared spectrometer (type MINISCAN IR LOG - AMETEK).

2.2.2. Lime characterization

The Agilent Model 55B AA flame atomic absorption spectrometer was used for the determination of calcium in the lime samples.

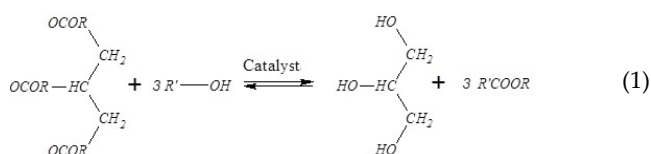
X-ray fluorescence spectrometry was employed for the identification and determination of chemical elements in concentration ranges from a few ppm to 100%.

2.3. Biodiesel synthesis

2.3.1. Synthesis protocol

The synthesis of biodiesel was carried out using transesterification, reaction of an alcohol and fatty ester which is catalyzed, usually by a base or an acid in homogeneous or heterogeneous catalysis to form esters of this alcohol and glycerine. The fatty esters consist of triglycerides solid at room temperature in the case of fats; and liquid at room temperature in the case of oils [4].

The transesterification reaction is written according to Eq. (1):



The biodiesel synthesis protocol developed in the laboratory followed the scheme represented in Fig. 1.

A quantity of catalyst (CaO) was dissolved in a volume of methanol. The heterogeneous mixture was then stirred vigorously for at least half an hour at room temperature since the reaction was exothermic. Subsequently, the used edible oil was poured into the mixture (methanol, catalyst) under continuous stirring. The mixture was heated at different temperatures and reaction times according to the experimental plan. Once the reaction was completed, it was followed by phase separation and washing (purification) of the allyl esters obtained. The separation of the phases (allyl esters phase and glycerin phase) took place as soon as agitation was stopped. The mixture was left to decant for 24 h for better separation.

The transesterification reaction resulted in two phases. The glycerol which had a higher density than the ester was the lower phase of the heterogeneous mixture. The lower phase (glycerin phase) was removed and the allyl ester upper phase was purified by a water wash to remove residual alcohol and traces of the catalyst. After the first washing with citric acid and then with distilled water, the appearance of two phases was observed: a cloudy lower phase and a yellowish upper phase (biodiesel). To obtain a better separation, the ester/water mixture was left to decant. The operation was repeated until the water phase became clear indicating complete removal of contaminants. The production of the esters was completed by drying in an oven at 80°C for 60 min to remove excess wash water and alcohol.

2.3.2. Transesterification yield of alkyl esters

The conversion rate [Eq. (2)] calculated the mass yield of the product.

$$Y(\%) = \left(\frac{\text{mass of the alkyl esters}}{\text{initial oil mass}} \right) \times 100 \quad (2)$$

2.3.3. Parametric study of transesterification reaction

Several parameters influence the yield and purity of methyl esters formed. These included the reaction time, the operating temperature, and the amount of catalyst. Table 1 shows the variations in the parameters employed in the optimization process. Using a fixed amount of used edible oil (30 g) and methanol (8 g), the effect of these three parameters

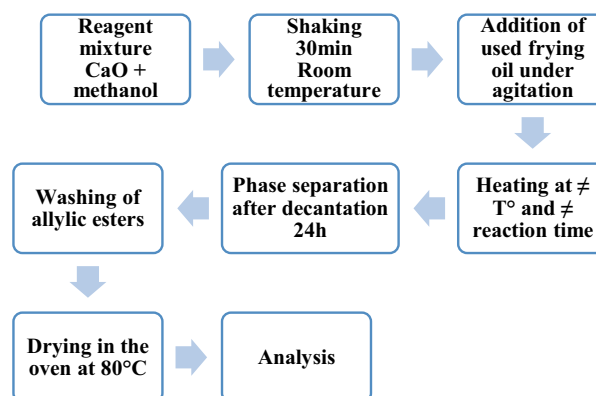


Fig. 1. Biodiesel synthesis protocol.

on methyl ester formation was studied and the results were analyzed.

2.3.4. Experimental design

Three factors were considered at three levels. It was a face centered composite design: central composite face centered (CCF). In this type of plan, the experimental domain was cubic. Each factor required 3 levels which were -1 , 0 , and 1 . The coding of the working domain for these three factors is presented in Table 2. The resolution associated with the model was performed using an 18-trial matrix method, which was necessary for the determination of the parameters expressing an optimal response.

Eighteen trials were conducted to test the influence of the factors on the optimization of the transformation yield and to ensure the convergence of the system towards an optimum point.

3. Results and discussion

3.1. Characterization of raw material

3.1.1. Characterization of the used oil

The physical and chemical characterization of used oil as well as that of fossil diesel and Food Codex Standards are described in Table 3. The viscosity of used frying oil (UFO) at 40°C was very high compared to conventional diesel, which would be a handicap for its direct use as biofuel. It was therefore imperative to reduce its viscosity to a value like that of conventional diesel (i.e., $1.5\text{--}4.5\text{ mm}^2/\text{s}$) since this has an influence on the quality of the fuel spray. The lower the viscosity the more finely the product would be atomized. This will optimize the fuel/air mixture, resulting in a better operation of the diesel engine. The density of UFO was within the range of the density standard of vegetable oils which varied from 0.915 to 0.964 but it was higher than that of fossil diesel. The latter indicates the degree of unsaturation, the state of oxidation or polymerization of the oil. The acidity index measured for the used cooking oil was below the maximum limit set by the standard [2.2–7.26]. As the free acid content of fats increased with time as a result of the hydrolysis reaction of UFOs. The acidity index was a tool to assess the state of deterioration of these fats. The more the acidity level increased, the less the yield of the transesterification reaction, which subsequently favored the reverse process (saponification).

The spectrum obtained by the FTIR analysis is shown in Fig. 2. By referring to the existing data banks in infrared spectrometry and considering the absorption bands of the obtained peaks, it was possible to identify the characteristic groups and bonds of the used frying oil:

- The carbonyl groups ($\text{C}=\text{O}$) present at the level of the chains extremities of the esters of fatty acids highlight an absorption band in the vicinity of $1,742\text{ cm}^{-1}$;
- The double bond ($\text{C}=\text{C}$) which characterizes the unsaturation of the fatty acids contained in the UFO, shows an absorption band towards $1,464\text{ cm}^{-1}$;
- The ether groups ($\text{C}-\text{O}-\text{C}$) show a corresponding peak at $1,152\text{ cm}^{-1}$;
- The groups ($-\text{CH}_2-$) characterizing the long aliphatic chains of the fatty acids (alkanes) have a band of average intensity of 721 cm^{-1} ;
- The ($-\text{CH}_2-$) groups at the adsorption band are located between $3,000$ and $2,860\text{ cm}^{-1}$.
- A strong adsorption band at $3,470\text{ cm}^{-1}$ is attributed to the ($-\text{OH}$) group.

3.1.2. Lime characterization

The technique of atomic spectroscopy was used to determine the concentration of calcium (element to be determined) in our commercial catalyst by measuring its absorption in lime. Based on the calibration curve developed, the mass percentage of calcium in the lime is 66% . Hence, the results clearly show that the quicklime or calcium oxide has a high calcium content which is about 66% . The active element in the composition of the catalyst which is in the form of calcium oxide (CaO). With its basic character it reacts with the methanol to form the methoxide anion which in its role effectively catalyzes the transesterification reaction.

The results of the quantitative analysis are reported in Table 4. The sample emitted 3 lines of the following composition: calcium 70.35% , which is the majority element, followed by magnesium 27.07% and chlorine 2.58% . The results obtained confirmed those previously obtained by SAA.

3.2. Parametric study of factors affecting transesterification yield

3.2.1. Effect of temperature of reaction environment

Temperature was a very important parameter in the yield and modulation of the transesterification reaction rate. The evolution of the transformation of UFO into methyl esters was carried out under the following operating conditions: a mass of 0.9 g of catalyst (CaO) and a reaction time of 24 h . This transformation was studied at different temperatures: 25°C , 40°C , 50°C , and 60°C . Fig. 3 shows the influence of temperature on the yield of methyl esters during the transesterification reaction of UFO. These experimental results showed that the conversion rate of UFO to methyl esters was low at temperatures below 40°C and improved with increasing temperature, until reaching a maximum of 69% , at a temperature

Table 1
Variation of the parameters to be studied

Parameter to be studied	Variation of the parameter
Reaction time (h)	24–48–72
Temperature of the reaction medium ($^{\circ}\text{C}$)	24–40–50–60
Catalyst quantity (g)	0.6–0.9–1.2

Table 2
Association of the factors to the coded variables of the experimental design

Factor (x_i)	Low level: -1	Center: 0	High level: $+1$
Temperature T ($^{\circ}\text{C}$)	40	50	60–1
Reaction time (h)	24	48	72
Catalyst quantity (g)	0.6	0.9	1.2

Table 3
Physico-chemical characteristics of used frying oil (UFO) and Food Codex Standard, 1999

Physico-chemical characteristics	UFO	Fossil diesel	Food Codex Standard
Viscosity at 20°C (mm ² /s)	46.17	–	
Viscosity at 40°C (mm ² /s)	34.67	1.5 at 4.5	
Density at 20°C	0.9164	0.82	0.913–0.932
Refractive index	1.4784	–	1.463–1.478
Acid value (mg-KOH/g)	2.805	–	2.2–7.26
Peroxide value	19	–	5.2–7.0
PCS (kJ/kg)	39	45.40	–
Flash point (°C)	204	≥55	220–350
Cloud point (°C)	–9		–
Pour point (°C)	–11		–

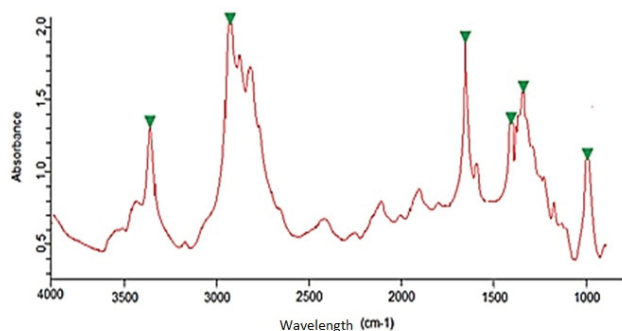


Fig. 2. Infrared spectrum of used frying oil.

Table 4
Chemical composition of quicklime

Element	Concentration (%)
Ca	70.35
Cl	2.58
Mg	27.07

between 40°C and 50°C. Above 50°C, the yield decreased. The amount of methanol present in the liquid reaction medium was slightly lower due to its evaporation (i.e., the boiling temperature of methanol being 65°C).

3.2.2. Effect of the quantity of catalyst used

Fig. 4 highlights the effect of catalyst on the transesterification reaction at 50°C for 24 h. It was found that increasing the amount of catalyst in the reaction gave better conversion yields. The best yield was 69% obtained for a reaction with 0.9 g of catalyst. An increase in the catalyst mass beyond this value led to a slight decrease in the yield. Indeed, a large amount of catalyst in the reaction led to the formation of soap and consequently to a reduction in the yield of the conversion of triglycerides into methyl esters.

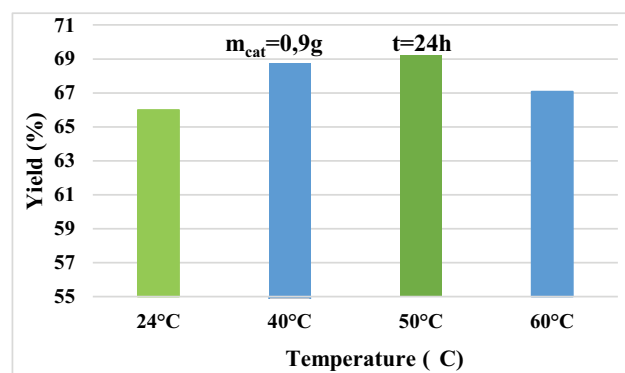


Fig. 3. Effect of temperature on the yield of the transesterification reaction.

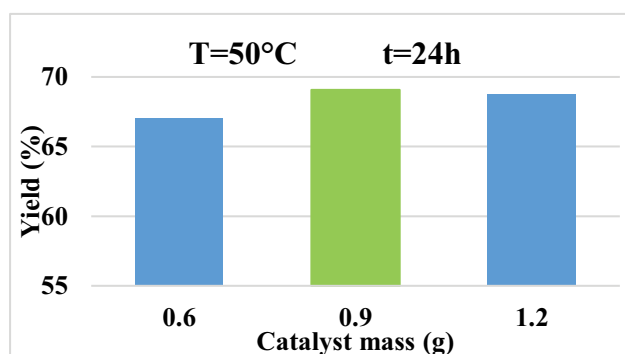


Fig. 4. Effect of catalyst mass on yield of transesterification reaction.

3.2.3. Effect of reaction time

For the determination of the optimal yield of methanoic transesterification, the reaction time was investigated using 0.9 g catalyst (CaO) at a temperature of 50°C. Fig. 5 shows that 66% of the methyl esters were produced after 24 h of reaction. Indeed, at the beginning, the reaction proceeded slowly because of the high viscosity of the mixture and the low solubility of the reactants. Once the reaction

was triggered, the products were more miscible with methanol and less viscous, which favored a rapid reaction. After more than 24 h almost all the oil was transformed into methyl esters for a maximum conversion rate of 75.72%. A reaction time of more than 48 h led to a lower yield.

3.3. Experimental design study

3.3.1. Physico-chemical properties of synthesized biodiesels

The physicochemical characteristics of the methyl esters must be compared with the standards in force applied to the quality control of these products. Therefore, after transesterification of UFO by basic catalysis and using methanol as alcohol, the products were subjected to physicochemical characterizations. Table 5 shows the results of the different characteristics obtained for the UFO methyl esters. The biodiesel produced by methanoic transesterification

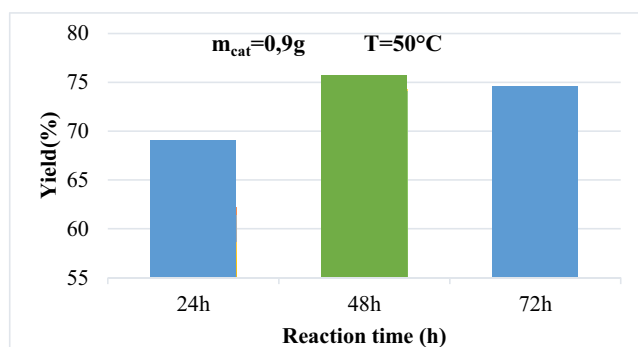


Fig. 5. Effect of reaction time on transesterification yield.

Table 5

Physico-chemical characteristics obtained for the UFO methyl esters from the experimental design

	N°	m_{CaO} (g)	T (°C)	Time (h)	Density	Viscosity at 20°C	Viscosity at 40°C	Flash point (°C)	Calorific value	Acidity index	Cloud point
Full factorial design	1	0.6	40	24	0.9111	13.99	5.54	189.19	35.08	1.568	-10.9
	2	1.2	40	24	0.911	13.5	5.35	182.66	36.97	1.514	-10.6
	3	0.6	60	24	0.911	13.63	5.4	184.33	36.48	1.528	-10.7
	4	1.2	60	24	0.9112	14.05	5.56	189.98	34.84	1.575	-11
	5	0.6	40	72	0.8919	12.35	4.89	167.1	41.49	1.385	-9.7
	6	1.2	40	72	0.9037	12.52	4.96	169.31	40.85	1.404	-9.8
	7	0.6	60	72	0.9074	12.77	5.06	172.73	39.85	1.432	-10
	8	1.2	60	72	0.9109	13.12	5.2	177.39	38.5	1.471	-10.3
	9	0.6	50	48	0.8984	12.45	4.93	168.33	41.13	1.395	-9.7
Axial points	10	1.2	50	48	0.9104	13.1	5.19	177.13	38.58	1.468	-10.3
	11	0.9	40	48	0.8273	11.46	4.54	155	45	1.285	-9
	12	0.9	60	48	0.874	12.11	4.8	163.74	42.46	1.357	-9.5
	13	0.9	50	24	0.9	12.47	4.94	168.61	41.05	1.398	-9.7
Repeats in center	14	0.9	50	72	0.8392	11.62	4.61	157.23	44.35	1.303	-9.1
	15	0.9	50	48	0.8431	11.68	4.63	157.97	44.14	1.31	-9.1
	16	0.9	50	48	0.8431	11.68	4.63	158.03	44.12	1.31	-9.2
	17	0.9	50	48	0.8435	11.7	4.63	158.21	44.07	1.312	-9.2
	18	0.9	50	48	0.8439	11.72	4.64	158.48	43.99	1.314	-9.2

had properties, that were comparable to international standards (EN14214, ASTM D6751).

Fig. 6 showed the different infrared spectra of biodiesel from HFU. The spectra had approximately the same appearance and the majority of the peaks were identical, which allowed for the identification of the characteristic peaks: an intense peak around 1,747 cm^{-1} attributed to the carbonyl group C=O of the ester function and then a strong absorption band located between 1,400–1,300 cm^{-1} associated with the asymmetrical elongation of the C–O–C functional groups. The spectra obtained also showed other peaks attributed to a possible presence of UFO. This was quite normal because biodiesel was derived from this oil. Conversion and purification are never perfect.

3.3.2. Yield of synthesized biodiesels

The results of the experimental design for the synthesis of biodiesel by transesterification of waste cooking oils were summarized grouped in Table 6. The optimal yield in biodiesel was obtained for the trial 11 which corresponded to values of the parameters of coordinates: reduced (0, -1, 0); real ($m_{CaO} = 0.9$ g, $T = 40^\circ\text{C}$, time = 48 h). On the other hand, the values obtained for the trials corresponding to the center replications showed good reproducibility of the results.

Comparing the yield values obtained for the trials where two parameters were identical while the third was varied, gave the following results. Biodiesel yield varied negatively with mass for maximum time (=72 h), while it varied positively for minimum and average times (=24 and 48 h, respectively). The yield varied positively with temperature for the minimum and average values, while for the maximum value it varied negatively. The variation of time had

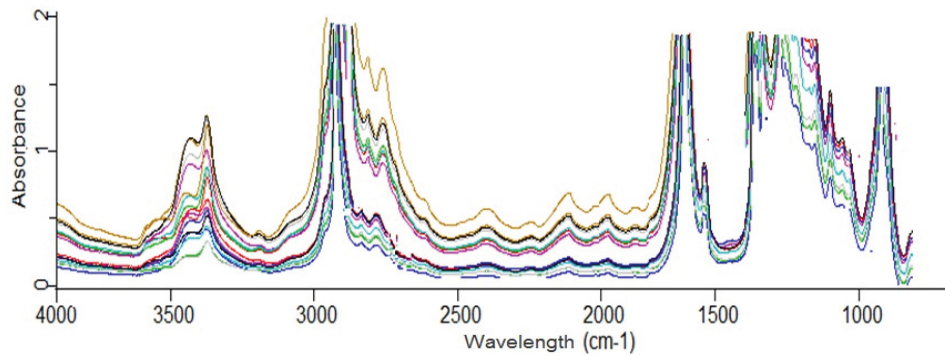


Fig. 6. Infrared spectra of different biodiesels from the UFO.

Table 6
Operating conditions and biodiesel yields obtained for the central composite design trials

	Trial	Real variables			Reduced variables			Yield Y (%)
		m_{CaO} (g)	T (°C)	Time (h)	A	B	C	
Full factorial design	1	0.6	40	24	-1	-1	-1	59.02
	2	1.2	40	24	+1	-1	-1	62.21
	3	0.6	60	24	-1	+1	-1	61.39
	4	1.2	60	24	+1	+1	-1	58.63
	5	0.6	40	72	-1	-1	+1	69.81
	6	1.2	40	72	+1	-1	+1	68.73
	7	0.6	60	72	-1	+1	+1	67.06
	8	1.2	60	72	+1	+1	+1	64.78
Axial points	9	0.6	50	48	-1	0	0	69.21
	10	1.2	50	48	+1	0	0	64.91
	11	0.9	40	48	0	-1	0	75.72
	12	0.9	60	48	0	+1	0	71.45
	13	0.9	50	24	0	0	-1	69.07
	14	0.9	50	72	0	0	+1	74.63
Repeats in the center	15	0.9	50	48	0	0	0	74.27
	16	0.9	50	48	0	0	0	74.24
	17	0.9	50	48	0	0	0	74.15
	18	0.9	50	48	0	0	0	74.02

a negative effect on the biodiesel yield when the mass was maximum ($m_{CaO} = 1.2$ g). On the other hand, for minimum and average mass the yield varied positively with time.

The processing of the results was carried out by STATGRAPHICS® software. The aim was to determine the different effects of each parameter, whether simple, quadratic or interaction, and to develop a model that described the behavior of the system. Analysis of variance is an important technique for analyzing the effect of qualitative factors on a response. An ANOVA (analysis of variance) breaks down the variability of the response according to the different factors. The determination of the significant factors was done using the null hypothesis noted H_0 which assumed that the effect of the parameter was equal to zero. The probability of accepting this hypothesis was noted Val-P.

- If $Val-P < 5\%$, the H_0 hypothesis was rejected and the parameter was significant.
- If $Val-P > 5\%$, the H_0 hypothesis was accepted and the parameter was not significant.

The results of the analysis of variance are given in Table 7. We can notice that the simple effects of time and temperature parameters are significant. It can be observed that among the quadratic effects, the time effect and the mass of the calcium oxide were significant. These results were represented by the Pareto chart, shown in Fig. 7. It showed that the parameters had a significant effect if they exceeded the value symbolized by the vertical line with a 5% risk of error.

The model proposed by the software was given in variables coded by the following equation:

$$\begin{aligned}
 \text{Yield} = & 74.2083 + 0.723m\text{CaO} - 1.218T + 3.469\text{Time} \\
 & - 7.18667m\text{CaO}^2 - 0.89375m\text{CaO} \times T \\
 & - 0.47375m\text{CaO} \times \text{Time} - 0.661667T^2 \\
 & - 0.68625 \times T \times \text{Time} - 2.39667 \times \text{Time}^2
 \end{aligned} \tag{3}$$

The coefficient indicating the goodness of fit of the estimates of the regression equation R^2 was equal to 97.90% and an adjusted R^2 equal to 95.74% which meant that the model described well the system studied.

Comparison of the experimental values of the yield with the values predicted by the model are shown in Table 8. The results indicated that the values were close for the 18 trials and that its estimated experimental error σ_2 did not exceed 1.186%. Therefore, the model fit was satisfactory and

Table 7
Analysis of variance

Parameter	P-value
A: m_{CaO}	0.0900
B:T	0.0117
C:Time	0.0000
AA	0.0000
AB	0.0657
AC	0.2913
BB	0.3853
BC	0.1404
CC	0.0104

Table 8
Experimental and calculated biodiesel yield values

	Trial	Yield Y (%)		
		Experimental values	Calculated values	Relative error
Full factorial design	1	59.02	60.38	-0.02304
	2	62.21	61.67	0.00868
	3	61.39	61.11	0.00456
	4	58.63	58.82	-0.00324
	5	69.81	69.64	0.00244
	6	68.73	69.03	-0.00436
	7	67.06	67.62	-0.00835
	8	64.78	63.44	0.02069
	9	69.21	67.74	0.02124
	10	64.91	66.30	-0.02141
Axial points	11	75.72	74.76	0.01268
	12	71.45	72.33	-0.01232
	13	69.07	68.34	0.01057
	14	74.63	75.28	-0.00871
Repeats in the center	15	74.27	74.21	0.00081
	16	74.24	74.21	0.00040
	17	74.15	74.21	-0.00081
	18	74.02	74.21	-0.00257

described well the system behavior.

The response surfaces were represented in a three-dimensional space showing the evolution of the response as a function of two parameters, the third being taken at its central level (zero level) (Fig. 8). The response surfaces allowed for detection of the experimental areas for an optimal response. The response surface corresponding to the mass-temperature couple illustrated in Fig. 8a shows that the yield increased with the amount of catalyst and was optimal when the latter was at its central level. However, a high temperature had a negative effect on the reaction yield. The evolution of the yield according to the mass-time represented by Fig. 8b indicates that at 50°C the yield increased with time and reached its optimum when the time was at its maximum level for an average quantity of catalyst (0.9 g in real variables). The representation of the yield in the time-temperature plane (Fig. 8c) confirmed a positive variation of the biodiesel yield with time. Moreover, it was evident that the yield increased with increasing temperature, for values between (-1,0) in coded variable (optimal value). Beyond this value, the trend

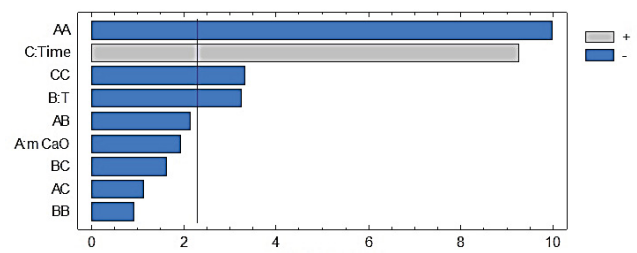


Fig. 7. Pareto chart.

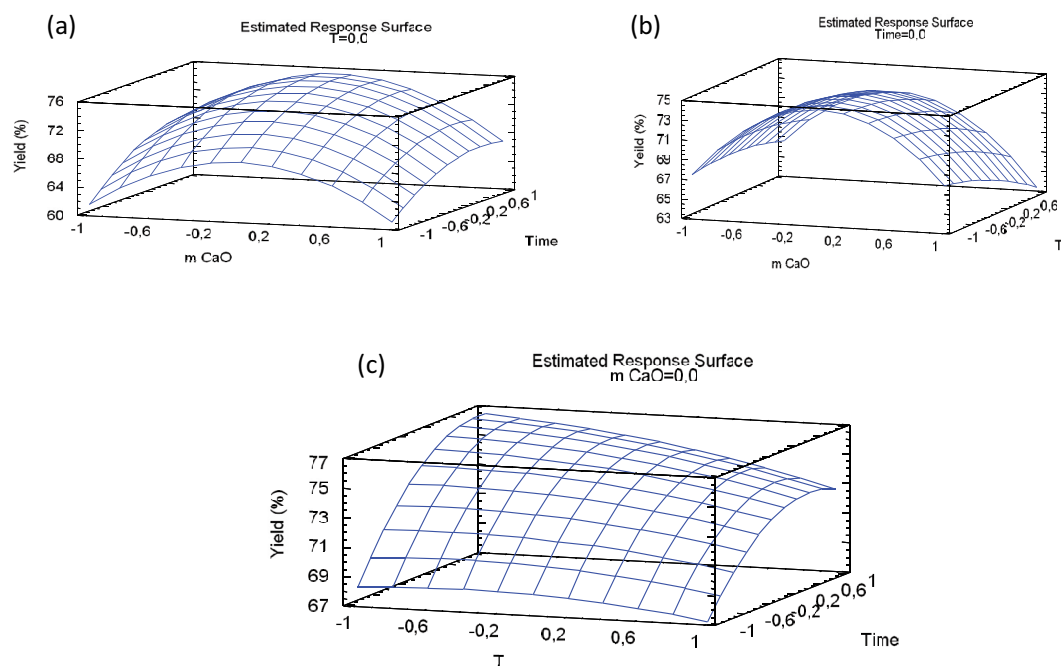


Fig. 8. Response surface.

Table 9
Experimental and statistical estimated optimal operating conditions

Optimal operating conditions			
Experimental		Estimated	
Real variables	Reduced variables	Real variables	Reduced variables
$m_{\text{CaO}} = 0.9 \text{ g}$	$m_{\text{CaO}} = 0$	$m_{\text{CaO}} = 0.895 \text{ g}$	$m_{\text{CaO}} = -0.0167411$
$T = 40^\circ\text{C}$	$T = -1$	$T = 40.000001^\circ\text{C}$	$T = -0.999999$
Time = 48 h	Time = 0	Time = 68.85 h	Time = 0.86858

was reversed. Table 9 shows that the experimental optimum was different from that estimated by the STATGRAPHICS® software on the time parameter.

4. Conclusions

The optimization of the used frying oil transesterification process using design of experiments was successfully optimized. Mathematical models describing the process as well as optimal conditions for the operating parameters were determined. The optimization of this process allowed for the identification of the optimal conditions ensuring both a maximum yield of bio-oil and an acceptable viscosity.

Current development models are based on the exploitation and use of fossil fuels. However, this petroleum-based material is polluting and non-renewable. The interest is therefore in turning to biofuels, energy materials derived from biomass, and which constitute an alternative, and a possible substitute for fossil fuels. The choice of used frying oil as a raw material in the synthesis of biodiesel was dictated by the inedible nature of the oil and its abundance.

The physico-chemical characteristics of this food waste are suitable for energy use. In its pure state in an engine, this oil is not feasible because of its very high viscosity of the order of $34.67 \text{ mm}^2/\text{s}$. Hence a chemical treatment was necessary to reduce this viscosity. Biofuels present a multitude of advantages, in particular renewability and non-toxicity.

References

- [1] United Nations Department of Economic and Social Affairs, Population Division, World Population Prospects 2022: Summary of Results, UN DESA/POP/2022/TR/NO. 3, New York, 2022.
- [2] K. Silpa, Y. Lisa, B.T. Perinaz, V.W. Frank, What a Waste 2.0: A Global Snapshot of Solid Waste Management to 2050. Urban Development, World Bank, Washington, D.C., 2018.
- [3] The Future of Life on Earth – Peak Oil, 18 août 2022, pp. 39–41. Available at: www.peakoil.net
- [4] I. Chapman, The end of Peak Oil? Why this topic is still relevant despite recent denials, Energy Policy, 64 (2014) 93–101.
- [5] D.B. Yacobucci, Alternative Fuels and Advanced Technology Vehicles: Issues in Congress, DIANE Publishing, Washington, 2013.

- [6] A. Demirbas, Progress and recent trends in biofuels, *Prog. Energy Combust. Sci.*, 33 (2007) 1–18.
- [7] A.E. Atabani, A.S. Silitonga, I.A. Badruddin, T.M.I. Mahlia, H.H. Masjuki, S. Mekhilef, A comprehensive review on biodiesel as an alternative energy resource and its characteristics, *Renewable Sustainable Energy Rev.*, 16 (2012) 2070–2093.
- [8] P. Shinoj, S.S. Raju, P.K. Joshi, India's biofuels production programme: need for prioritizing the alternative options, *Indian J. Agric. Sci.*, 81 (2011) 391–397.
- [9] A.H. Hirani, N. Javed, M. Asif, S.K. Basu, A. Kumar, A Review on First- and Second-Generation Biofuel Productions, A. Kumar, S. Ogita, Y.Y. Yau, Eds., *Biofuels: Greenhouse Gas Mitigation and Global Warming*, Springer, New Delhi, 2018, pp. 141–154. Available at: https://doi.org/10.1007/978-81-322-3763-1_8
- [10] D. Ballerini, N. Alazard-Toux, *les Biocarburants, États de lieux, Perspectives et enjeux du développement*, Institut Français du Pétrole (IFP), Technip, France, 2006, p. 348.
- [11] M.E. Günay, L. Türker, N. Alper Tapan, Significant parameters and technological advancements in biodiesel production systems, *Fuel*, 250 (2019) 27–41.
- [12] T.A. Andrade, M. Errico, K.V. Christensen, Influence of the reaction conditions on the enzyme catalyzed transesterification of castor oil: a possible step in biodiesel production, *Bioresour. Technol.*, 243 (2017) 366–374.
- [13] F. Ferella, G. Mazziotti Di Celso, I. De Michelis, V. Stanisci, F. Vegliò, Optimization of the transesterification reaction in biodiesel production, *Fuel*, 89 (2010) 36–42.
- [14] T. Ahmad, M. Danish, P. Kale, B. Geremew, S.B. Adeloju, M. Nizami, M. Ayoub, Optimization of process variables for biodiesel production by transesterification of flaxseed oil and produced biodiesel characterizations, *Renewable Energy*, 139 (2019) 1272–1280.
- [15] S.A. Anand Kumar, G. Sakthinathan, R. Vignesh, J. Rajesh Banu, A.H. Al-Muhtaseb, Optimized transesterification reaction for efficient biodiesel production using Indian oil sardine fish as feedstock, *Fuel*, 253 (2019) 921–929.
- [16] K. Thakkar, S.S. Kachhwaha, P. Kodgire, Multi-response optimization of transesterification reaction for biodiesel production from castor oil assisted by hydrodynamic cavitation, *Fuel*, 308 (2022) 121907, doi: 10.1016/j.fuel.2021.121907.
- [17] S.K. Nayak, A.T. Hoang, B. Nayak, P.C. Mishra, Influence of fish oil and waste cooking oil as post mixed binary biodiesel blends on performance improvement and emission reduction in diesel engine, *Fuel*, 289 (2021) 119948, doi: 10.1016/j.fuel.2020.119948.
- [18] Standard Test Method for Density of Semi-Solid and Solid Asphalt Materials (Nickel Crucible Method), Normes américaines ASTM, 2017, ASTM D3289-17.
- [19] Standard Test Method for Kinematic Viscosity of Transparent and Opaque Liquids (and Calculation of Dynamic Viscosity), Normes américaines ASTM, 2021, ASTM D 445.
- [20] Corps gras d'origines animale et végétale – Détermination de l'indice d'acide et de l'acidité. Normes internationales ISO, 2020, ISO 660:2020.
- [21] Standard Test Method for Heat of Combustion of Liquid Hydrocarbon Fuels by Bomb Calorimeter, Normes américaines ASTM, 2020, ASTM D 240.
- [22] Corps gras d'origines animale et végétale – Détermination de l'indice de peroxyde – Détermination avec point d'arrêt iodométrique, Normes nationales et documents normatifs nationaux, 2017, NF EN ISO 3960.
- [23] Corps gras d'origines animale et végétale – Détermination de l'indice de réfraction, Normes nationales et documents normatifs nationaux, 2017, NF EN ISO 6320.
- [24] Produits pétroliers – Point d'éclair en vase clos des lubrifiants et des huiles combustibles, Normes nationales et documents normatifs nationaux, 1986, NF T60-103.
- [25] Produits pétroliers – Détermination du point de trouble, Normes nationales et documents normatifs nationaux, ISO 3015:1992.
- [26] Produits pétroliers – Détermination du point d'écoulement, Normes nationales et documents normatifs nationaux, 1996, NF T60-105.